Vietnam Journal of Mechanics, Vol. 46, No. 1 (2024), pp. 44 – 57
DOI: https://doi.org/10.15625/0866-7136/20580

DYNAMIC RESPONSE OF SANDWICH BEAM WITH POROUS CORE EXCITED BY TWO HARMONIC LOADS TRAVELLING IN OPPOSITE DIRECTIONS

Tran Quang Hung[1], **Do Minh Duc**[1,*], **Tran Minh Tu**[2]
[1]*The University of Da Nang - University of Science and Technology, Da Nang, Vietnam*
[2]*Hanoi University of Civil Engineering, Hanoi, Vietnam*
E-mail: ducdhbk@gmail.com

Received: 23 January 2024 / Revised: 02 March 2024 / Accepted: 12 March 2024
Published online: 31 March 2024

Abstract. This paper presents the time history response of a sandwich beam with a porous core subjected to two moving harmonic loads with opposite directions. In the modelling, the beam is combined of two isotropic face sheets and a porous core with symmetric porosity distribution. The quasi-3D shear deformation beam theory in conjunction with Hamilton's variational principle is utilized to set up the governing equations of motion. The Navier solution is used to obtain the displacement field. The accuracy of the study is validated by comparing with existing results in the literature for specific cases. Effects of the velocity and excitation frequency of the moving loads on the deflection-time history are investigated and discussed. Numerical results reveal that in the case of the double-moving harmonic loads in the antiphase, the resonance phenomenon cannot occur when the excitation frequency approaches the natural frequency of the beam.

Keywords: sandwich porous beam, moving harmonic load, Navier solution, dynamic response.

1. INTRODUCTION

Lightweight sandwich structures with a porous core offer unique potential for various applications in space/aerospace, automotive, defense and civil engineering [1]. In these structures, the porous core plays a prime key since it has many advantages, such as high energy absorption ability, high resistance to impact, high strength- and stiffness-to-weight ratios [2, 3]. Consequently, this type of structure has gained the attention of

the scientific community. Chen et al. [3] investigated the effect of geometric nonlinearity and shear deformation on the free vibration of sandwich beams with a porous core. Wang et al. [4] studied the nonlinear bending of a sandwich beam with composite face sheets and a closed-cell porous core subjected to a distributed load by the equivalent single-layer model. Srikarun et al. [5] investigated the linear and nonlinear bending of sandwich beams with a metal foam core under different types of distributed loads. Wang and Zhao [6] explored the effects of porosity and elastic foundation on the natural frequencies of the sandwich beam with a metal foam core. Garg et al. [7] reported the free vibration and static bending of sandwich beams containing open-cell metal foam core by zigzag theory.

The dynamics of structures subjected to moving loads is one of the interesting topics for exploring mechanical behaviour. Furthermore, specific mechanical knowledge related to this problem is important for many engineering applications, such as bridges, guideways, railroads, overhead cranes, and gun-tubes. It is found in the literature that the vibration characteristics of structures under moving loads have been studied for well over a century. Recently, this research topic has focused on structures with advanced materials, such as functionally graded material (FGM), porous materials, materials reinforced with graphene platelets (GPLs)/carbon nanotubes (CNTs), etc. Zhang et al. [8] presented the DSC regularized Dirac-delta method for the vibration analysis of GPL reinforced porous beams resting on an elastic foundation under a moving load. Songsuwan et al. [9] examined effect of the geometrical nonlinearity on the vibration of sandwich beams with a porous core under the action of a moving load. Simsek [10] analyzed the dynamic behavior of a FGM beam under a moving mass with different beam theories. Jafari and Kiani [11] focused on the dynamic response of porous beams reinforced with GPLs subjected to a moving load by using the quasi-3D theory. Van-Long Nguyen et al. [12] investigated the nonlinear dynamic features of porous beams interacted with the Winkler–Pasternak foundation and subjected to a travelling mass. Yas and Heshmati [13] dealt with the transient response of nanocomposite beams reinforced with CNTs under a moving load by the finite element method.

The researches mentioned-above refer to the single moving load. In fact, structures may undergo multi-moving loads with different values of velocity. Consequently, the dynamic response as well as the mathematical modelling of the problem becomes more complicated. A number of studies have also attempted to address and provide insight into this situation. Heshmati and Yas [14] presented the dynamic behaviour of nanocomposite beams reinforced with CNTs subjected to multi-moving loads. Wattanasakulpong et al. [15] examined the nonlinear response of polymer beams reinforced with GPLs and excited by two moving loads. Simsek and Al-shujairi [16] analyzed the forced vibration

of FGM sandwich beams excited by two moving harmonic loads. Using the mesh-free approach, Sayyidmousavi et al. [17] simulated the dynamic response of polymer sandwich beams reinforced with CNTs and subjected to two moving harmonic loads.

The literature survey shows that studies on the dynamic response of porous beam subjected to moving harmonic loads are in the beginning stage and the results are still limited. No report is found in the case of the beams subjected to two loads travelling in opposite directions. Moreover, effects of two moving harmonic loads with different excitation on the dynamic response of the beams is worth exploring to gain an insight into mechanical issues. Therefore, this study makes an attempt to simulate and investigate dynamic behaviour of a sandwich beam with a metal foam core subjected to two moving harmonic loads with opposite directions. Importantly, the analytical solution and the quasi-3D theory are utilized to model the system. The rest of the paper is organized as follows: Section 2 introduces the theoretical modelling of the sandwich beam; Section 3 is devoted to a validation study and investigation into the significant parameters on the dynamic response of the beam; finally, Section 5 is for summaries and conclusions of new findings derived from the numerical results.

2. THEORY AND MATHEMATICAL MODELLING

Fig. 1 illustrates a porous sandwich beam under two moving loads in opposite directions. The two loads depart from the two ends of the beam at the same time. The three dimensions of the beam are the length L, width b, and thickness h. The x-axis of the coordinate system is on the mid-plane of the beam. The configuration of the studied beam is composed of two isotropic skins and an open-cell metal foam core with a symmetric porosity distribution. The thicknesses of the skins and the core are h_f and h_c, respectively. It is assumed in the current study that there is no relative sliding between the layers as well as the collision of the moving loads.

2.1. Material property modelling

The configuration of the sandwich beam is composed of three layers. The face ones are made of isotropic and homogeneous material. Whereas, the core one contains pores and their effective material properties strongly depend on the porosity distributions. Various types of porosity distribution scheme are proposed by authors in the literature. Previous studies show that the symmetric distribution of a high density of pores around the middle zone and a lower density of pores near the faces of the porous layer exhibits the highest structural stiffness. Thus, this porosity distribution is adopted for the studied beam. According to this view, the effective mechanical properties can be modelled along

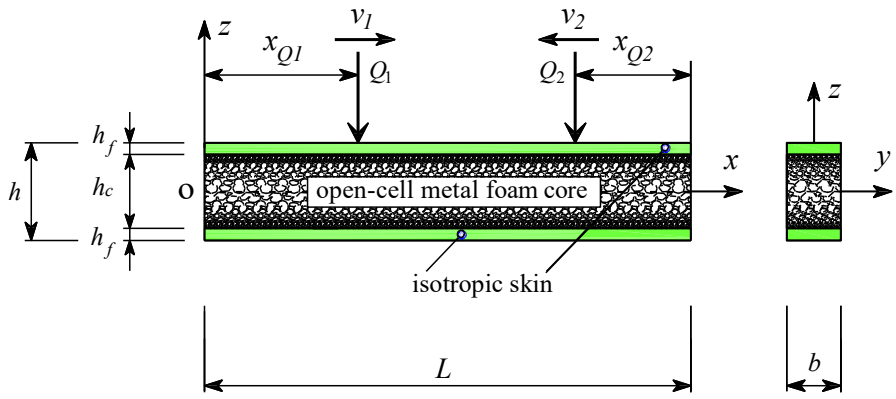

Fig. 1. Configuration and geometry parameters of a porous sandwich beam subjected to two moving loads with opposite directions

the thickness of the beam by the following expression

For the face layers:

$$\begin{cases} E(z) = E_f, \\ \rho(z) = \rho_f, \\ -0.5h \le z \le -0.5h_c \cup 0.5h_c \le z \le 0.5h, \end{cases}$$

For the porous core:

$$\begin{cases} E(z) = E_c\left[1 - \vartheta_o \cos\left(\pi z/h_c\right)\right], \\ \rho(z) = \rho_c\left[1 - \vartheta_m \cos\left(\pi z/h_c\right)\right], \\ -0.5h_c \le z \le 0.5h_c, \end{cases} \tag{1}$$

where E_f and ρ_f are, respectively, Young's modulus and mass density of the material of the faces. E_c and ρ_c are those of the core without any pores (pure material); ϑ_o and ϑ_m indicate the porosity coefficient and the coefficient of mass density, respectively ϑ_m can be determined via ϑ_o by the relation [3] $\vartheta_m = 1 - \sqrt{1 - \vartheta_o}$.

2.2. Kinematics

In this study, the quasi-3D beam theory, which includes both the shear deformation and thickness stretching effect, is employed. Based on this beam theory, the displacement field $u(x,z,t)$, $w(x,z,t)$, along the x- and z-directions, can be described as [18]

$$\begin{cases} u(x,z,t) = u_o(x,t) - z w_{o,x}(x,t) + \Phi(z)\,\theta_{os}(x,t) \\ w(x,z,t) = w_o(x,t) + \Phi_{,z}(z)\,w_{oz}(x,t), \end{cases} \tag{2}$$

where u_o, w_o, w_{oz} and θ_{os} are four variable displacements on the mid-plane; Φ is the shape function which characterizes the distribution of the shear strain over the beam thickness. The third-order function $\Phi(z) = z - 4z^3/(3h^2)$ is selected for this study.

The strain field can be given as follows

$$\begin{cases} \varepsilon_x = u_{,x} = u_{o,x} - zw_{o,xx} + \Phi\theta_{os,x}, \\ \varepsilon_z = w_{,z} = \Phi_{,zz} w_{oz}, \\ \gamma_{xz} = u_{,z} + w_{,x} = \Phi_{,z}\left(\theta_{os} + w_{oz,x}\right). \end{cases} \tag{3}$$

The stress-strain relation obeys the Hooke's law:

$$\boldsymbol{\sigma} = \begin{Bmatrix} \sigma_x \\ \sigma_z \\ \tau_{xz} \end{Bmatrix} = \begin{bmatrix} Q_{11} & Q_{12} & 0 \\ Q_{21} & Q_{22} & 0 \\ 0 & 0 & Q_{33} \end{bmatrix} \begin{Bmatrix} \varepsilon_x \\ \varepsilon_z \\ \gamma_{xz} \end{Bmatrix}. \tag{4}$$

The elastic coefficients in Eq. (4) are given as

$$Q_{11} = Q_{22} = \frac{E(z)}{1-v^2}, \quad Q_{12} = Q_{21} = vQ_{11}, \quad Q_{33} = \frac{E(z)}{2(1+v)}, \tag{5}$$

where v is the Poisson's ratio of the materials and assumed not to depend on the porosity in this study.

2.3. Energy expressions and governing equations

The variation of strain energy δU of the beam due to the stresses can be evaluated by

$$\delta U = \int_0^L \int_A \left(\sigma_x \delta\varepsilon_x + \sigma_z \delta\varepsilon_z + \tau_{xz}\delta\gamma_{xz}\right) \mathrm{d}A\mathrm{d}x, \tag{6}$$

$$\delta U = \int_0^L \left[N_x u_{o,x} - M_B \delta w_{o,xx} + M_S \delta\theta_{os,x} + R_z \delta w_{oz} + Q\left(\delta\theta_{os} + \delta w_{oz,x}\right)\right] \mathrm{d}x, \tag{7}$$

in which the stress resultants are defined by

$$\left\{N_x, M_B, M_S, Q, R_z\right\} = \int_A \left\{\sigma_x, \sigma_x z, \sigma_x \Phi\left(z\right), \tau_{xz}\Phi_{,z}\left(z\right), \sigma_z \Phi_{,zz}\left(z\right)\right\} \mathrm{d}A, \tag{8}$$

where A is the area of the beam cross-section, and L is the beam length.

The stress resultants can be expressed via the displacements by employing Eqs. (2) and (4) as

$$\begin{Bmatrix} N_x \\ M_B \\ M_S \\ R_z \\ Q \end{Bmatrix} = \begin{bmatrix} A & -B & B_S & C_1 & 0 \\ B & -D & D_S & C_2 & 0 \\ B_S & -D_S & H_S & C_3 & 0 \\ C_1 & -C_2 & C_3 & C_4 & 0 \\ 0 & 0 & 0 & 0 & A_S \end{bmatrix} \begin{Bmatrix} u_{o,x} \\ w_{o,xx} \\ \theta_{os,x} \\ w_{oz} \\ \theta_{os} + w_{oz,x} \end{Bmatrix}, \tag{9}$$

in which

$$\{A, B, B_S, D, D_S, H_S\} = \int_A Q_{11} \left\{1, z, \Phi, z^2, z\Phi, \Phi^2\right\} \mathrm{d}A, \tag{10}$$

$$\{C_1, C_2, C_3, C_4, A_S\} = \int_A Q_{11} v \left\{\Phi_{,zz}, z\Phi_{,zz}, \Phi\Phi_{,zz}, \frac{1}{v}\left(\Phi_{,zz}\right)^2, \frac{(1-v)}{2v}\left(\Phi_{,z}\right)^2\right\} \mathrm{d}A. \tag{11}$$

The variation of kinetic energy δK of the sandwich beam due to the motion can be determined by

$$\delta K = \int_0^L \int_A \rho\left(z\right)\left(\dot{u}\delta\dot{u} + \dot{w}\delta\dot{w}\right) \mathrm{d}A\mathrm{d}x. \tag{12}$$

Substituting Eq. (2) into Eq. (12) results in

$$\begin{aligned}\delta K = &\int_0^L \left[I_o(\dot{u}_o\delta\dot{u}_o + \dot{w}_o\delta\dot{w}_o) - I_1\left(\dot{u}_o\delta\dot{w}_{o,x} + \dot{w}_{o,x}\delta\dot{u}_o\right) + I_2\dot{w}_{o,x}\delta\dot{w}_{o.x} + J_1\left(\dot{u}_o\delta\dot{\theta}_{os} + \dot{\theta}_{os}\delta\dot{u}_o\right)\right]\mathrm{d}x \\ &+ \int_0^L \left[-J_2\left(\dot{w}_{o,x}\delta\dot{\theta}_{os} + \dot{\theta}_{os}\delta\dot{w}_{o,x}\right) + J_3\dot{\theta}_{os}\delta\dot{\theta}_{os} + J_4\left(\dot{w}_o\delta\dot{w}_{oz} + \dot{w}_{oz}\delta\dot{w}_o\right) + J_5\dot{w}_{oz}\delta\dot{w}_{oz}\right]\mathrm{d}x,\end{aligned} \tag{13}$$

where

$$\{I_o, I_1, I_2, J_1, J_2, J_3, J_4, J_5\} = \int_A \rho\left(z\right)\left\{1, z, z^2, \Phi, z\Phi, \Phi^2, \Phi_{,z}, \left(\Phi_{,z}\right)^2\right\} \mathrm{d}A. \tag{14}$$

Finally, the variation of the work due to the distributed load $q(x, t)$ can be determined by

$$\delta V = -\int_0^L q\left(x, t\right)\delta w_o. \tag{15}$$

To obtain the the governing equations, the following Hamilton's principle [19] can be used

$$\int_{t_1}^{t_2} (\delta K - \delta U - \delta V)\mathrm{d}t = 0. \tag{16}$$

By substituting $\delta U, \delta K$ and δV from Eqs. (7), (13) and (15) into Eq. (16), then performing the integration by parts and collecting the coefficients of δu_o, δw_o, $\delta\theta_{os}$ and δw_{oz},

the governing equations of motion of the sandwich beam can be obtained as follows

$$\begin{cases} Au_{o,xx} - Bw_{o,xxx} + B_S\theta_{os,xx} + C_1 w_{oz,x} = I_o\ddot{u}_o - I_1\ddot{w}_{o,x} + J_1\ddot{\theta}_{os}, \\ Bu_{o,xxx} - Dw_{o,xxxx} + D_S\theta_{os,xxx} + C_2 w_{oz,xx} + q = I_1\ddot{u}_{o,x} + I_o\ddot{w}_o - I_2\ddot{w}_{o,xx} + J_2\ddot{\theta}_{os,x} + J_4\ddot{w}_{oz}, \\ B_S u_{o,xx} - D_S w_{o,xxx} + H_S\theta_{os,xx} + C_3 w_{oz,x} - A_S\left(\theta_{os} + w_{oz,x}\right) = J_1\ddot{u}_o - J_2\ddot{w}_{o,x} + J_3\ddot{\theta}_{os}, \\ -C_1 u_{o,x} + C_2 w_{o,xx} - C_3\theta_{os,x} - C_4 w_{oz} + A_S\left(\theta_{os,x} + w_{oz,xx}\right) = J_4\ddot{w}_o + J_5\ddot{w}_{oz}. \end{cases} \tag{17}$$

3. NAVIER SOLUTION

Eq. (17) can be solved by using Navier solution for the case of the beam with the simply supported conditions. Assuming the four unknowns have been expanded to the trigonometric series as follows

$$\begin{cases} u_o\left(x,t\right) = \sum\limits_{n=1}^{\infty} U_n\left(t\right)\cos\left(\lambda_n x\right), \; w_o\left(x,t\right) = \sum\limits_{n=1}^{\infty} W_n\left(t\right)\sin\left(\lambda_n x\right), \\ \theta_{os}\left(x,t\right) = \sum\limits_{n=1}^{\infty} \Theta_n\left(t\right)\cos\left(\lambda_n x\right), \; w_{oz}\left(x,t\right) = \sum\limits_{n=1}^{\infty} W_{zn}\left(t\right)\sin\left(\lambda_n x\right), \; \lambda_n = n\pi/L, \end{cases} \tag{18}$$

where U_n, W_n, Θ_n and W_{zn} are the time-dependent unknown coefficients that become the alternative variables of the problem; n is the term of the series.

When the two concentrated moving harmonic loads $Q_1 = Q_o\sin(\Omega_1 t + \phi_1)$ and $Q_2 = Q_o\sin(\Omega_2 t + \phi_2)$ are applied on the beam as illustrated in Fig. 1, they may be written as [11]

$$q\left(x,t\right) = \begin{cases} \sum\limits_{n=1}^{\infty} Q_n^1\left(t\right)\sin\left(\lambda_n x\right), \;\; Q_n^1\left(t\right) = \dfrac{2Q_1}{L}\sin\left(\lambda_n x_{Q1}\right) & \text{for moving load } Q_1, \\ \sum\limits_{n=1}^{\infty} Q_n^2\left(t\right)\sin\left(\lambda_n x\right), \;\; Q_n^2\left(t\right) = \dfrac{2Q_2}{L}\sin\left(\lambda_n L - \lambda_n x_{Q2}\right) & \text{for moving load } Q_2, \end{cases} \tag{19}$$

where Q_o is the amplitude of the moving harmonic loads, Ω_1 and Ω_2 are the excitation frequencies, ϕ_1 and ϕ_2 indicate the phase angles, x_{Q1} and x_{Q2} are the locations of the moving loads.

By substituting Eqs. (18) and (19) into Eq. (17) we obtain

$$\mathbf{KX} + \mathbf{M}\ddot{\mathbf{X}} = \mathbf{F}. \tag{20}$$

The explicit form of the matrices and vectors of Eq. (20) are

$$\mathbf{K} = \begin{bmatrix} k_{11} & k_{12} & k_{13} & k_{14} \\ & k_{22} & k_{23} & k_{24} \\ & & k_{33} & k_{34} \\ \text{sym.} & & & k_{44} \end{bmatrix}, \quad \mathbf{M} = \begin{bmatrix} m_{11} & m_{12} & m_{13} & m_{14} \\ & m_{22} & m_{23} & m_{24} \\ & & m_{33} & m_{34} \\ \text{sym.} & & & m_{44} \end{bmatrix},$$
$$\mathbf{F} = \begin{Bmatrix} 0 \\ -Q_n^1 - Q_n^2 \\ 0 \\ 0 \end{Bmatrix}, \quad \mathbf{X} = \begin{Bmatrix} U_n \\ W_n \\ \Theta_n \\ W_{zn} \end{Bmatrix}, \tag{21}$$

The components in the matrices **K** and **M** are defined by

$$\begin{aligned} &k_{11} = -\lambda_n^2 A, \quad k_{12} = \lambda_n^3 B, \quad k_{13} = -\lambda_n^2 B_S, \quad k_{14} = \lambda_n C_1, \quad k_{22} = -\lambda_n^4 D, \quad k_{23} = \lambda_n^3 D_S, \\ &k_{24} = -\lambda_n^2 C_2, \quad k_{33} = -\lambda_n^2 H_S - A_S, \quad k_{34} = \lambda_n C_3 - \lambda_n A_S, \quad k_{44} = -C_4 - \lambda_n^2 A_S, \\ &m_{11} = -I_o, \quad m_{12} = \lambda_n I_1, \quad m_{13} = -J_1, \quad m_{14} = 0, \quad m_{22} = -I_o - \lambda_n^2 I_2, \quad m_{23} = \lambda_n J_2, \\ &m_{24} = -J_4, \quad m_{33} = -J_3, \quad m_{34} = 0, \quad m_{44} = -J_5. \end{aligned} \tag{22}$$

Eq. (20) can be reduced to the equation of free vibration with the natural frequency ω as follows

$$\left(\mathbf{K} - \omega^2 \mathbf{M}\right) \mathbf{X} = \mathbf{0}. \tag{23}$$

4. NUMERICAL EXAMPLES

4.1. Validation study

Firstly, the first three dimensionless natural frequencies $\left(\omega_i L/h\sqrt{12\rho/E}\right)$ of the an isotropic homogeneous beam are computed and compared with those of Jafari and Kiani [11] based on the quasi-3D beam theory. Parameters of the beam are set as $E_f = E_c = E$, $\rho_f = \rho_c = \rho$, $\upsilon_f = \upsilon_c = \upsilon = 0.3$ [11], $\vartheta_o = 0.0$. The dimensionless natural frequencies are listed in Table 1. As can be seen, the present results completely agree with those of Jafari and Kiani [11].

The second validation is conducted for the porous sandwich beam which is composed as steel/steel foam/steel. The free vibration of this beam type was performed by Songsuwan et al. [9]. Material properties the skins and the core are $E_f = E_c = 200$ GPa, $\rho_f = \rho_c = 7850$ kg/m^3, $\upsilon_f = \upsilon_c = 0.3$ [9]. The values of the first dimensionless frequency with different values of L/h ratio are illustrated in Table 2. The data in Table 2 show that the numerical results of the different sources are matched very well. The present results are slightly lower than those of other authors due the use of different beam theories. The present study uses the quasi-3D beam model while Songsuwan et al. [9] used the higher-order beam theory (HOBT) in their work.

Table 1. Comparison of the first three dimensionless frequencies of a homogeneous beam

L/h	Sources	Theory	Mode 1	Mode 2	Mode 3
2	Present	Quasi-3D	7.4703	20.5256	34.3054
	Jafari and Kiani [11]	Quasi-3D	7.4703	20.5256	34.3054
5	Present	Quasi-3D	9.2905	32.3474	62.0692
	Jafari and Kiani [11]	Quasi-3D	9.2905	32.3474	62.0692
10	Present	Quasi-3D	9.7121	37.1619	78.4339
	Jafari and Kiani [11]	Quasi-3D	9.7121	37.1619	78.4339

Table 2. Comparison of the first dimensionless frequency $\widehat{\omega}_1 = \omega_1 L\sqrt{\rho_c\left(1-v_c^2\right)/E_c}$ of the porous sandwich beam ($\vartheta_o = 0.5$, $h_c/h_f = 10$)

L/h	Sources	Theories	$\widehat{\omega}_1$	L/h	Sources	Theories	$\widehat{\omega}_1$
20	Present	Quasi-3D	0.1391	40	Present	Quasi-3D	0.0699
	[9]	HOBT	0.1457	40	[9]	HOBT	0.0732
30	Present	Quasi-3D	0.0930	50	Present	Quasi-3D	0.0559
	[9]	HOBT	0.0975	50	[9]	HOBT	0.0586

The third validation is devoted to the time-dependent response of a solid and homogeneous beam with single layer by eliminating the two skin layers and setting $e_o = 0$. The beam is subjected to one moving load (without the excitation frequency) of magnitude Q_o and constant velocity v. Assuming the deflection and velocity of the system are equal to zero at $t = 0$, and neglecting the structural damping. The analytical formulation of the deflection for the simply-supported (SS) beam and based on the classical beam theory can be presented as [20]

$$\begin{cases} w\left(x,t\right) = \sum\limits_{i=1}^{n} \dfrac{1}{\rho bhL} \times \dfrac{2Q_o}{\omega_i^2 - \left(i\pi v/L\right)^2} \times \left[\sin\left(\dfrac{i\pi vt}{L}\right) - \dfrac{i\pi v}{\omega_i^L}\sin\left(\omega_i^t\right)\right] \times \sin\left(\dfrac{i\pi x}{L}\right), \\ \omega_i = i^2\pi^2\sqrt{Eh^2/\left(12\rho L^4\right)}, \quad i = 1,2,...,n \end{cases} \tag{24}$$

The deflection at the center of the beam versus the time is plotted in Fig. 2. The dimensionless deflection is used as $\hat{w} = 48Ebh^3w/\left(12Q_oL^3\right)$ for the presentation. For the aim of validation, this deflection is calculated by two approaches: (a) by the analytical formulation, i.e., Eq. (24); and (b) by the Navier solution, i.e., Eq. (20), with Newmark-β method. The time step size is selected as 5×10^{-3} seconds. Parameters of the studied case are $L = 8$ m, $L/h = 40$, $v = 8$ m/s. The width of the beam is unity. Material properties

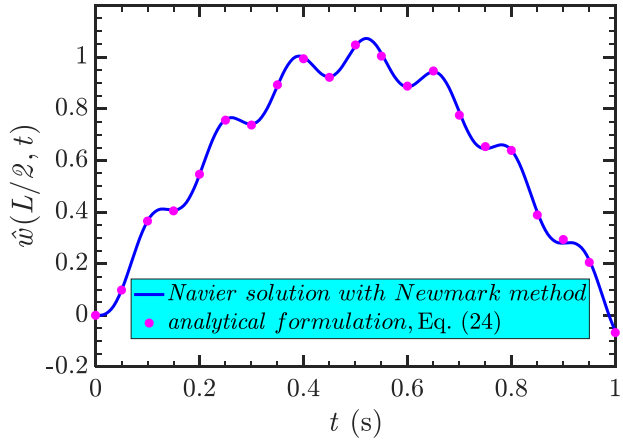

Fig. 2. Dimensionless time-dependent deflection at the center of an isotropic SS beam based on the Navier solution and the analytical formulation

of the beam are: $E = 70$ GPa, $\rho = 2702$ kg/m^3, $v = 0.3$. It should be noted that the excitation of the moving load is not included by setting $\sin(\Omega t + \phi) = 1$.

As observed in Fig. 2, the deflections calculated by two approaches are in good agreement, which confirms the reliability of the developed model.

4.2. Parametric study

In this part, the porous sandwich beam which is layered as Aluminum/Aluminum foam/Aluminum is concerned. The length of the beam is $L = 8$ m, the width is unity, and $L/h = 40$. Material properties are: $E_f = E_c = 70$ GPa, $\rho_f = \rho_c = 2702$ kg/m^3, $v_f = v_c = 0.3$. For the Newmark integration, the initial deflection and initial velocity are equal to zero, and the size of the time-step is 5×10^{-3} seconds. The dimensionless deflection is defined as the third validation ($\hat{w}(x,t) = 48Ebh^3 w(x,h/2,t)/12Q_o L^3$) and is used in the presentation.

As the beam is subjected to moving loads, the deflection at a section changes over the time. Fig. 3 plots the dimensionless maximum deflection at the sections along the beam length ($|\hat{w}|_{\max}(x/L)$) with different values of porosity coefficient (e_o) when the beam is excited by two loads travelling in the opposite directions along the length. Two moving harmonic loads with the same excitation frequency ($\Omega_1 = \Omega_2 = 25$ rad/s), and zero phase angles ($\phi_1 = \phi_2 = 0$), but different velocities are concerned in this investigation. It can be observed from the figure that when e_o increases, the deflection increases because the stiffness of the beam decreases; increasing v_2 leads to reduce the maximum deflection. Interestingly, in the cases of $e_o = 0.0$ or $e_o = 0.8$ combined with $v_2 = 4$ m/s, the maximum values of $|\hat{w}|_{\max}(x/L)$are not at the middle span of the beam.

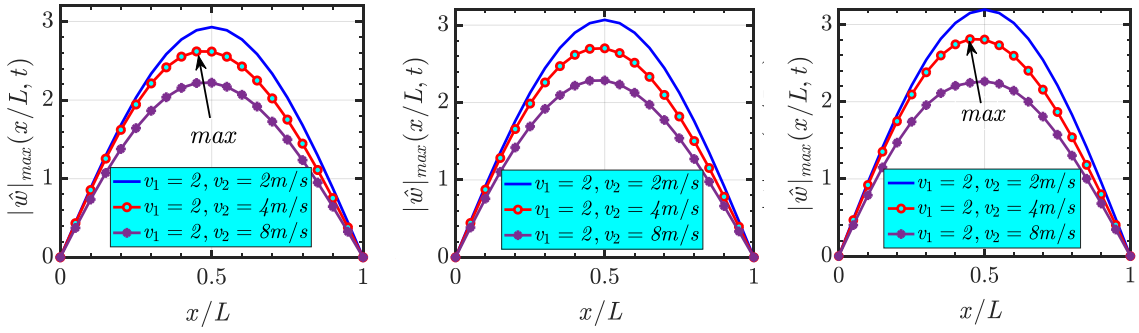

(a) $e_o = 0.0$ (b) $e_o = 0.4$ (c) $e_o = 0.8$

Fig. 3. Maximum dimensionless deflection along the beam with different values of the porosity coefficient and moving load velocity ($h_c/h_f = 8$, $L/h = 40$, $\Omega_1 = \Omega_2 = 25$ rad/s, $\phi_1 = \phi_2 = 0$)

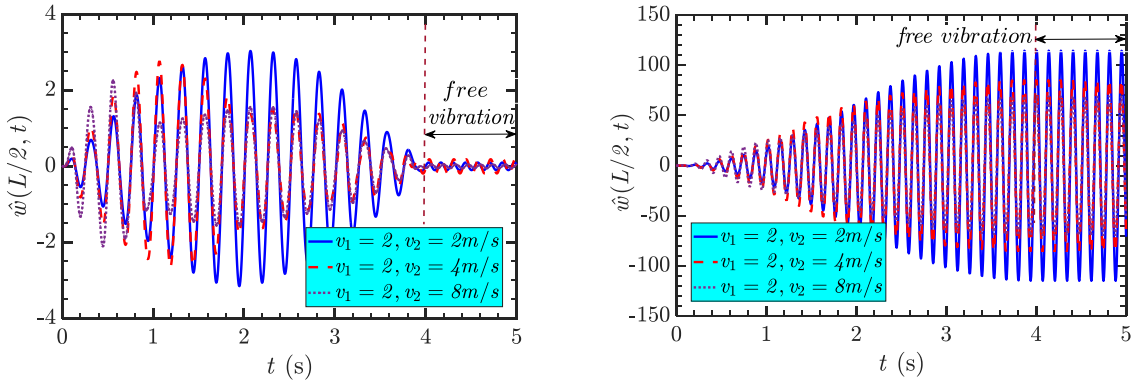

(a) $\Omega_1 = \Omega_2 = 25$ rad/s (b) $\Omega_1 = \Omega_2 = 46$ rad/s

Fig. 4. Dimensionless time-dependent deflection at the center of the beam with different values of the excitation frequency and moving load velocity ($h_c/h_f = 8$, $L/h = 40$, $e_o = 0.5$, $\phi_1 = \phi_2 = 0$)

Fig. 4 depicts the dimensionless time-dependent deflection at the center of the beam with two cases of the excitation frequency combined with three sets of moving load velocities. We also examine the dynamic response of the beam for one second after all the loads leave the beam (free vibration phase). As seen from the results in Fig. 4 when $v_2 > v_1$, the oscillation amplitude decreases sharply (compared with the case $v_2 = v_1$) after the moving load with v_2 leaves the beam. This is because the beam then carries less load. As expected, when the excitation frequency approaches the fundamental frequency of the beam ($\Omega_1 = \Omega_2 = 46.0 \approx \omega_1 = 46.7347$ rad/s), the resonance phenomenon occurs; the oscillation amplitude increases rapidly and reaches very large deflection. Besides, in the free vibration phase, the oscillation amplitude does not change.

Fig. 5 aims to investigate the dynamic deflection in the resonance case ($\Omega_1 = \Omega_2 = 46.0 \approx \omega_1 = 46.7347$ rad/s), but different phase angles and different velocities of the two moving loads. Three sets of the phase angles ($\phi_1 = \phi_2 = 0$, $\phi_1 = 0$ and $\phi_2 = \pi$, $\phi_1 = \pi$ and $\phi_2 = 0$) combined with two sets of the moving load velocities ($v_1 = v_2 = 2$ m/s, $v_1 = 2$ m/s and $v_2 = 8$ m/s) are considered in the investigation. The figure shows that when the two moving loads are in the same phase ($\phi_1 = \phi_2 = 0$), the beam is then in the resonance situation with a very large dynamic deflection. However, in the other two cases ($\phi_1 = 0$ and $\phi_2 = \pi$, $\phi_1 = \pi$ and $\phi_2 = 0$), the two moving loads always act in opposite directions (in the antiphase) the oscillation amplitude is much smaller than the same phase in the case of $v_1 \neq v_2$ (see Fig. 5(b)) and the vibration is even eliminated in the case of $v_1 = v_2$ (see Fig. 5(a)). In addition, in the case $v_2 > v_1$ when the first load leaves the beam, the resonance phenomenon occurs again; the oscillation amplitude increases rapidly.

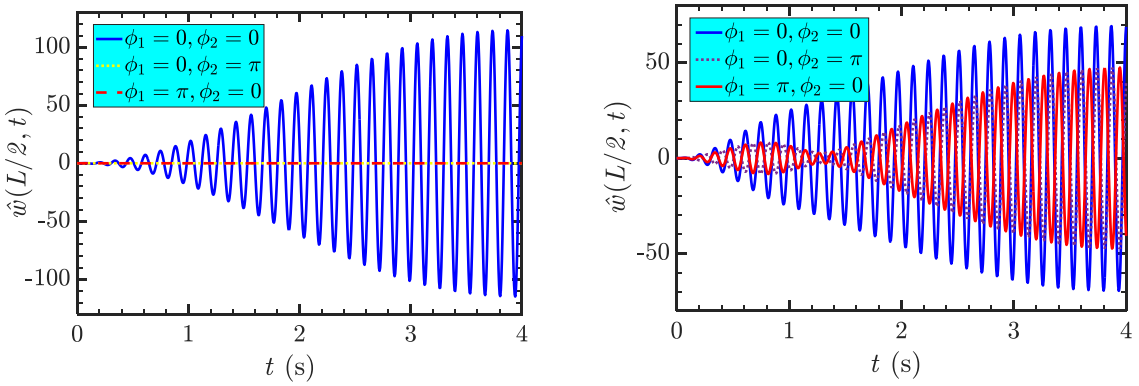

(a) $v_1 = 2$ m/s, $v_2 = 2$ m/s (b) $v_1 = 2$ m/s, $v_2 = 8$ m/s

Fig. 5. Dimensionless time-dependent deflection at the center of the beam in the resonance case, but different phase angles and velocities of the moving loads ($h_c/h_f = 8$, $L/h = 40$, $e_o = 0.5$)

5. CONCLUSIONS

The paper presents the dynamic response of a sandwich beam with a porous core excited by two harmonic loads travelling in opposite directions. The beam is composed of two isotropic face sheets and a porous core with symmetric porosity distribution. The quasi-3D shear deformation beam theory in conjunction with Hamilton's variational principle is utilized to derive the governing equations of motion. The Navier solution is used to obtain the explicit forms of the displacement field. The accuracy of the study is validated by comparing with existing results in the literature for specific cases. Effects of the velocity and excitation frequency of the moving loads on the deflection-time history

are investigated and discussed. The numerical results reveal that (1) the dynamic deflection is strongly affected by the combined velocities of two moving loads; (2) in the case of the double-moving harmonic loads with the same amplitude Q_o are in the antiphase, the resonance phenomenon cannot occur when the excitation frequency approaches the natural frequency of the beam.

DECLARATION OF COMPETING INTEREST

The authors declare that they have no known competing financial interests or personal relationships that could have appeared to influence the work reported in this paper.

ACKNOWLEDGMENTS

This research is funded by Vietnam's National Foundation for Science and Technology Development (NAFOSTED) under grant number: 107.02-2021.16

REFERENCES

[1] N. E. P. A. Gokhale and B. Basu. *Light weighting for defense, aerospace, and transportation*. Springer Singapore, (2019). https://doi.org/10.1007/978-981-15-1263-6.

[2] M. F. Ashby, A. Evans, N. A. Fleck, L. J. Gibson, J. W. Hutchinson, H. N. G. Wadley, and F. Delale. Metal foams: A design guide. *Applied Mechanics Reviews*, **54**, (2001), pp. B105–B106. https://doi.org/10.1115/1.1421119.

[3] D. Chen, S. Kitipornchai, and J. Yang. Nonlinear free vibration of shear deformable sandwich beam with a functionally graded porous core. *Thin-Walled Structures*, **107**, (2016), pp. 39–48. https://doi.org/10.1016/j.tws.2016.05.025.

[4] Y. Wang, H. Ma, K. Xie, T. Fu, J. Chen, and Y. Liu. Nonlinear bending of a sandwich beam with metal foam and GPLRC face-sheets using Chebyshev–Ritz method: Effects of agglomeration and internal pore. *Thin-Walled Structures*, **181**, (2022). https://doi.org/10.1016/j.tws.2022.110035.

[5] B. Srikarun, W. Songsuwan, and N. Wattanasakulpong. Linear and nonlinear static bending of sandwich beams with functionally graded porous core under different distributed loads. *Composite Structures*, **276**, (2021). https://doi.org/10.1016/j.compstruct.2021.114538.

[6] Y. Q. Wang and H. L. Zhao. Free vibration analysis of metal foam core sandwich beams on elastic foundation using Chebyshev collocation method. *Archive of Applied Mechanics*, **89**, (2019), pp. 2335–2349. https://doi.org/10.1007/s00419-019-01579-0.

[7] A. Garg, H. D. Chalak, M. O. Belarbi, and A. M. Zenkour. A parametric analysis of free vibration and bending behavior of sandwich beam containing an open-cell metal foam core. *Archives of Civil and Mechanical Engineering*, **22**, (2022). https://doi.org/10.1007/s43452-021-00368-3.

[8] L. H. Zhang, S. K. Lai, C. Wang, and J. Yang. DSC regularized Dirac-delta method for dynamic analysis of FG graphene platelet-reinforced porous beams on elastic foundation under a moving load. *Composite Structures*, **255**, (2021). https://doi.org/10.1016/j.compstruct.2020.112865.

[9] W. Songsuwan, N. Wattanasakulpong, and S. Kumar. Nonlinear transient response of sandwich beams with functionally graded porous core under moving load. *Engineering Analysis with Boundary Elements*, **155**, (2023), pp. 11–24. https://doi.org/10.1016/j.enganabound.2023.05.055.

[10] M. Şimşek. Vibration analysis of a functionally graded beam under a moving mass by using different beam theories. *Composite Structures*, **92**, (2010), pp. 904–917. https://doi.org/10.1016/j.compstruct.2009.09.030.

[11] P. Jafari and Y. Kiani. A four-variable shear and normal deformable quasi-3D beam model to analyze the free and forced vibrations of FG-GPLRC beams under moving load. *Acta Mechanica*, **233**, (2022), pp. 2797–2814. https://doi.org/10.1007/s00707-022-03256-w.

[12] V.-L. Nguyen, M.-T. Tran, T.-B. Chu, T.-A. Nguyen, and V.-L. Nguyen. Nonlinear dynamic response of functionally graded porous beams under a moving mass using Reddy's beam theory. *Iranian Journal of Science and Technology, Transactions of Mechanical Engineering*, (2023), pp. 1–17. https://doi.org/10.1007/s40997-023-00705-2.

[13] M. H. Yas and M. Heshmati. Dynamic analysis of functionally graded nanocomposite beams reinforced by randomly oriented carbon nanotube under the action of moving load. *Applied Mathematical Modelling*, **36**, (2012), pp. 1371–1394. https://doi.org/10.1016/j.apm.2011.08.037.

[14] M. Heshmati and M. H. Yas. Dynamic analysis of functionally graded multi-walled carbon nanotube-polystyrene nanocomposite beams subjected to multi-moving loads. *Materials & Design*, **49**, (2013), pp. 894–904. https://doi.org/10.1016/j.matdes.2013.01.073.

[15] N. Wattanasakulpong, A. Karamanli, and T. P. Vo. Nonlinear dynamic response of FG-GPLRC beams induced by two successive moving loads. *Engineering Analysis with Boundary Elements*, **159**, (2024), pp. 164–179. https://doi.org/10.1016/j.enganabound.2023.11.025.

[16] M. Şimşek and M. Al-shujairi. Static, free and forced vibration of functionally graded (FG) sandwich beams excited by two successive moving harmonic loads. *Composites Part B: Engineering*, **108**, (2017), pp. 18–34. https://doi.org/10.1016/j.compositesb.2016.09.098.

[17] A. Sayyidmousavi, M. Foroutan, and Z. Fawaz. Meshfree dynamic analysis of functionally graded carbon nanotube reinforced polymer sandwich beams under harmonic moving loads. *Australian Journal of Mechanical Engineering*, (2022), pp. 1–13. https://doi.org/10.1080/14484846.2022.2114157.

[18] A. S. Sayyad and Y. M. Ghugal. Modeling and analysis of functionally graded sandwich beams: a review. *Mechanics of Advanced Materials and Structures*, **26**, (2018), pp. 1776–1795. https://doi.org/10.1080/15376494.2018.1447178.

[19] J. N. Reddy. *Mechanics of laminated composite plates and shells*. CRC Press, (2003). https://doi.org/10.1201/b12409.

[20] M. M. Stanisić and J. C. Hardin. On the response of beams to an arbitrary number of concentrated moving masses. *Journal of the Franklin Institute*, **287**, (1969), pp. 115–123. https://doi.org/10.1016/0016-0032(69)90120-3.